Microscopic model for hysteresis and phase equilibria of fluids confined between parallel plates

U. Marini Bettolo Marconi
Dipartimento di Fisica, II Università di Roma "Tor Vergata," 00173 Roma, Italy

F. Van Swol
Department of Chemical Engineering, University of Illinois at Urbana–Champaign, Urbana, Illinois 61801
(Received 17 November 1988)

The hysteresis effects of fluids confined in porous media are studied by means of a new microscopic model. We consider a slitlike pore of infinite area and finite height. In contrast to the unbounded parallel-plate case, the new model allows the formation and the disappearance of curved menisci at the open ends of the pore. This effect has a profound influence on the extent of the hysteresis loops. On the other hand, we find that the presence of the menisci does not play a significant role in locating the equilibrium first-order transition in long pores. The present treatment reconciles the traditional picture of capillary condensation with the modern microscopic treatment based on the density-functional formalism.

I. INTRODUCTION

The properties of fluids confined in small systems have been a subject of active research as an application of concepts of statistical mechanics and thermodynamics. From the practical point of view these systems attract considerable attention because they serve as useful models for porous materials, i.e., objects with large specific surface area, which find applications in many industrial processes.

The theoretical study of porous media was initiated by Zsigmondy[1] and co-workers some 80 years ago. By applying the so-called Kelvin equation, Zsigmondy explained the condensation phenomenon, which occurs in these systems, and in addition provided one of the first theories of the adsorption hysteresis. It had been observed, in fact, that after inverting the direction of change of the applied pressure, during an adsorption experiment, the amount adsorbed often failed to retrace the values through which it passed during the forward process.

Subsequently, Cohan,[2] rejecting Zsigmondy's view that hysteresis was due to impurity effects, proposed a theory which still enjoys a great popularity. According to this theory the hysteresis was related to the different shapes of the menisci during the adsorption and the desorption process. The weakness of Cohan's theory is the use of a purely thermodynamical approach based on macroscopic concepts such as interfacial tension and dividing surface, the so-called meniscus, between liquid and gas phases. It is difficult to justify the use of these notions at length scales of the order of the mesopore size where one should employ only microscopic concepts.

The understanding of capillary phenomena was substantially advanced by the study of wetting behavior at interfaces during the last ten years.[3–5] The so-called van der Waals theory in particular, providing a method to deal successfully with inhomogeneous media, has stimulated the microscopic study of fluids in porous media.

Very recently Evans and co-workers[6–12] embarked upon the microscopic study of capillary phenomena, modeling pores by infinitely long cylinders or unbounded parallel plates. They showed that the effect of a finite distance between the plates and of adsorbing walls is to shift the bulk liquid-gas phase transition to a pressure which is below the saturated pressure, i.e., the value at coexistence. Their studies allow one to go beyond the classical macroscopic theory due to Kelvin and to investigate in detail the behavior of fluids in very narrow pores. In addition, they showed the existence of a new kind of second-order phase transition, termed capillary criticality. Among other merits, their theory gives the first detailed account of the observed first-order transition and of the sharp rise of the amount adsorbed during the imbibition process. On the other hand, according to their model one does not observe a steep decrease in the coverage, i.e., of the amount of adsorbed material, close to the condensation point, during the desorption process. This appears to be in contrast with the experimental findings. Thus the shape of the adsorption isotherm, as predicted by the model above, shows an upper part of the hysteresis loop which is too extended towards lower pressures and terminates only very close to the bulk spinodal, where the liquid phase becomes unstable against long wavelength fluctuations.

The main object of the present work is to illustrate the dramatic effects induced by the pore ends on the emptying of the system. We find that the liquidlike metastable states are strongly affected by the presence of pore ends and this fact eventually leads to their complete suppression and hence it explains why the emptying process occurs very close to the true equilibrium transition. As we shall show, on the basis of a fully self-consistent treatment, we are able to predict the desorption behavior starting from a microscopic approach. Moreover, when the size of the systems under study becomes large com-

pared with the molecular scale, the present theory allows one to recover the macroscopic picture.

In modeling the pore we consider the two plates unbounded only in one direction. The finite direction schematizes end effects, which determine the formation of a meniscus. To further investigate the hysteresis behavior we specialize to two kinds of models: Model A is s slit with both ends open and model B which has one end closed to mimic the so called wedge model and/or pore blocking effects. In order to carry out our calculations efficiently and to noticeably reduce the computational time involved, we have chosen to describe the fluid by means of the lattice gas model. In spite of its simplicity the present model is able to capture the salient features we want to illustrate. The present paper is organized as follows: in Sec. II we introduce the new model and give a brief outline of the theory, in Sec. III we illustrate the results, in Sec. IV we give a discussion, and in Sec. V we present the conclusions.

II. LATTICE-GAS MODEL FOR ADSORPTION

The lattice gas has been previously used to model the adsorption of fluids on a substrate,[13,14] capillary condensation in cylindrical pores,[15] and between parallel plates.[16] The lattice gas is described as a collection of N atoms, which can take up only discrete positions on a lattice structure formed by M sites. Each site, belonging to the lattice of coordination number f, can be occupied by at most one atom. The interaction between atoms is taken to be of the nearest-neighbor type, such that the interaction energy is $-\varepsilon$, if two atoms occupy contiguous sites. The system as a whole is in contact with a reservoir of particles at constant temperature T and chemical potential μ.

Here, we shall consider the lattice gas confined between walls. The single-wall potential is due to an assembly of *wall atoms,* which occupy the lattice sites of a parallelepiped, of edges, respectively, L_x, L_y, and L_z. The attractive interaction between the *wall atoms* and the lattice gas is assumed to be of the van der Waals $-1/r^6$ type. In the limit of $L_x \to \infty$ the external field due to a single wall is found to be

$$V^{\text{single}}(y,z) = -\frac{3\pi}{8}\alpha\varepsilon \sum_{y',z'} \left[\frac{\sigma^2}{(y-y')^2+(z-z')^2} \right]^{5/2} , \tag{2.1}$$

where α is a measure of the strength of the solid-fluid interaction and σ is the unit of length. In model A a second wall, identical and parallel to the first, was placed at a distance N_z. In addition, in order to mimic the reservoir filled with gas, the walls and the lattice gas are extended in the y direction by L_b sites. These sites represent the reservoir and the walls surrounding it consist of sites with an average occupancy set equal to that of the bulk gas. Their interaction with the lattice gas atoms has strength $-\varepsilon$ and is also of the nearest-neighbor type.

In model B, the partially closed pore, we have only a reservoir at one end. A third wall, similar to the ones previously described, closes the opposite end. The total external field V^{ext} equals the sum of the single-wall contributions plus the interaction of the reservoir particles with the boundaries of the reservoir.

The Hamiltonian is given by

$$H = -\frac{\varepsilon}{2} \sum_{i,j,l,i',j',l'} n_{i,j,l} n_{i',j',l'} + \sum_{i,j,l} V^{\text{ext}}(\mathbf{r}_{ijl}) n_{i,j,l} , \tag{2.2}$$

where $\mathbf{r}_{ijl}$ is the vector position of the site i,j,l and $n_{i,j,k}=1$ if the site is occupied and 0 if empty. The first summation runs over all nearest neighbor sites of the subsystem pore fluid plus reservoir fluid, whereas the second sum is over all sites.

In order to avoid spurious condensation effects we have chosen the dimension L_b of the reservoir larger than the bulk correlation length of the fluid. We have found that this precaution is sufficient to render our numerical results virtually independent on the choice of L_b, within the numerical precision required.

The chemical potential of an homogeneous lattice gas on a cubic lattice structure ($f=6$ nearest neighbors) at a temperature T is

$$\mu = k_B T \ln\left[\frac{n}{1-n}\right] - f\varepsilon n , \tag{2.3}$$

where n is the average occupancy and k_B is the Boltzmann factor and its pressure P is given by

$$P = k_B T[n \ln n + (1-n)\ln(1-n)] - f\varepsilon n^2/2 . \tag{2.4}$$

The appropriate quantity to consider in the grand canonical ensemble is the grand potential functional,[17] which within the mean-field approximation (MFA) reads

$$\Omega_V = k_B T \sum_{i,j,l} [\bar{n}_{i,j,l}\ln(\bar{n}_{i,j,l}) + (1-\bar{n}_{i,j,l})\ln(1-\bar{n}_{i,j,l})] - \frac{\varepsilon}{2} \sum_{i,j,l,i',j',l'} \bar{n}_{i,j,l}\bar{n}_{i',j',l'} + \sum_{i,j,l} [V^{\text{ext}}(\mathbf{r}_{ijl}) - \mu]\bar{n}_{i,j,l} , \tag{2.5}$$

where $\bar{n}_{i,j,l}$ is the average occupancy of the site i,j,l.

We obtained solutions for the problem by applying an iterative technique[16] to solve the Euler-Lagrange equation that results upon differentiating the grand potential functional (2.5),

$$\delta\Omega_V/\delta\bar{n}_{i,j,l} = 0 . \tag{2.6}$$

The following separation of Eq. (2.6) was chosen:

$$\bar{n}_{i,j,l} = \{1+\exp[(V^{\text{eff}}_{i,j,l}-\mu)/(k_B T)]\}^{-1} , \tag{2.7}$$

where $V^{\text{eff}}_{i,j,l} = V^{\text{ext}}_{i,j,l} + V^{\text{int}}_{i,j,l}$ and $V^{\text{int}}_{i,j,l}$ is the internal field at the site (i,j,l),

$$V^{\text{int}}_{i,j,l} = -\varepsilon \sum_{i',j',l'}{}' \bar{n}_{i',j',l'} , \tag{2.8}$$

where the primed sum is restricted to nearest-neighbor sites only.

Starting from an appropriate guess (we have chosen spatially uniform density profiles) for $\{\bar{n}_{i,j,l}\}$ one iterates Eq. (2.6) until a convergence criterion is satisfied.

III. RESULTS OF CALCULATIONS

Calculations were performed for several values of the wall potential strength parameter α, the chemical potential μ, the temperature T, and the height of the plates L_y. In order to emphasize the particular nature of the results obtained for the two models introduced above, we compared these with the corresponding predictions for the unbounded uniform slit.

As an order parameter we define the quantity

$$\Gamma = \frac{1}{L_z L_y N_z} \sum_{i,j,l} \bar{n}_{i,j,l} \ , \tag{3.1}$$

that is, the average density in the volume contained between the plates. A convenient measure of the distance from bulk two-phase coexistence is the paramer s, which we define as the ratio $n_{\rm gas}/n_{\rm gas}^{\rm coex}$. We begin to illustrate the results for $\alpha=4.512$ and $T/T_c=0.8$ and plate separation N_z equal to 18 layers. The unbounded slit (Fig. 1) shows the extended loops characteristic of this model.[16] The emptying process is due to a process of spinodal decomposition at $s=0.7$, very close to the bulk spinodal. A first-order phase transition between a *liquid* configuration and *gas* configuration occurs at $s=0.907$. The solution of the Euler-Lagrange equation (2.7) is stable for values of $s > s_{\rm spinodal}$. Only at this value the liquidlike solution turns from metastable unstable and the associated metastable minimum of the grand potential disappears. On the adsorption branch the coverage grows continuously and eventually as the pressure approaches the saturated pressure the film becomes unstable and the capillary becomes completely full with liquid.

We turn the attention to Fig. 2 which shows the adsorption isotherm for two plates having the same potential strength and being finite in the vertical direction ($L_z=140$). We observe that the adsorption process looks almost identical to the one which occurs in the infinite slit. In contrast, the desorption branch shows a novel character. The loop rounds off at a value of the saturation close to the condensation value and then decreases steeply in an almost continuous fashion, until it merges into the gas branch.

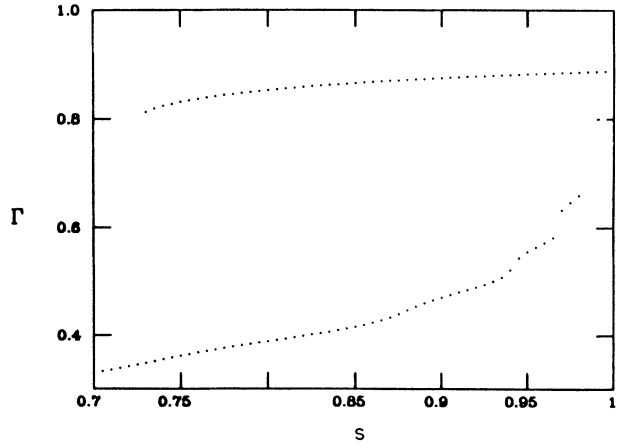

FIG. 1. Average occupancy Γ plotted against the undersaturation ratio $s=\rho_{\rm bulk}/\rho_{\rm gas}$ for an infinitely long slit of width $N_z=18$ at fixed temperature $T=0.8T_c$. The equilibrium phase transition takes place at $s=0.907$.

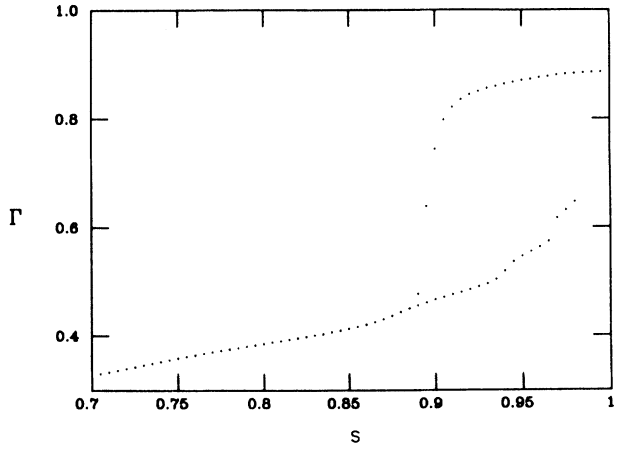

FIG. 2. Γ vs s for a slit of width $N_z=18$ and height $L_y=140$ at fixed temperature $T=0.8T_c$. The equilibrium phase transition takes place at $s=0.91$. Note the reduced length of the metastable portion of Γ along the liquid branch with respect to the infinitely long slit (Fig. 1).

We stress the fact that the first order transition, i.e., the point where *gas* and *liquid* coexist in the pore, is not located exactly where we observe a sharp decrease in the coverage, but at a value of the saturation slightly larger than that corresponding to condensation in the infinite plate case ($s=0.91$). This is a typical finite-size effect, which induces a correction of order H/l for large systems, as we shall discuss in Sec. IV. The width of the loop is roughly proportional to $2\gamma/H$, where γ is the liquid-gas surface tension.[18]

In Fig. 3 we illustrate the results for the partially closed pore. The desorption branch is almost indistinguishable from the open pore case. On the other hand, we do not find hysteresis and the adsorption is the same as the desorption. We remark that also some macroscopic theories, such as the one proposed by Cohan,[2] predict the absence of hysteresis in wedge shaped pores and in tapering capillaries. As we shall observe below the absence of hysteresis in model B occurs only at temperatures sufficiently high.

In Fig. 4 the contour profile obtained by plotting the locus of constant density $\rho=0.5$ is displayed. This contour yields a detailed insight into the capillary condensation phenomenon and provides a visualization of the meniscus, i.e. of the liquid-gas interface in a pore. Figure 4 shows a series of menisci obtained for series of values of the chemical potential. As the undersaturation increases one observes the meniscus to recede towards the center of the slit, until it changes shape. For a slit, finite in the vertical direction, the emptying seems to occur in a

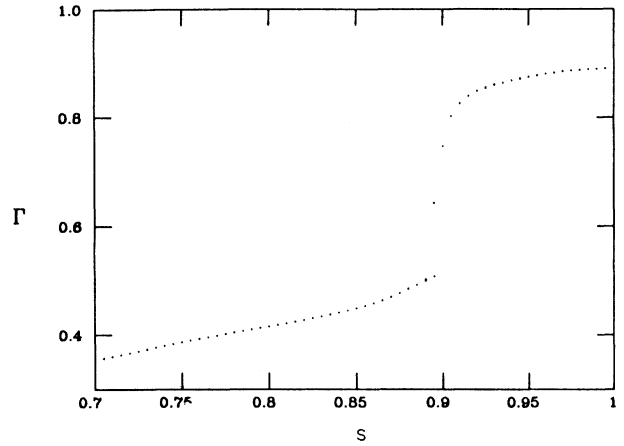

FIG. 3. Γ vs s for a partially closed slit of width $N_z=18$ and height $L_y=70$ at fixed temperature $T=0.8T_c$. Note the absence of hysteresis.

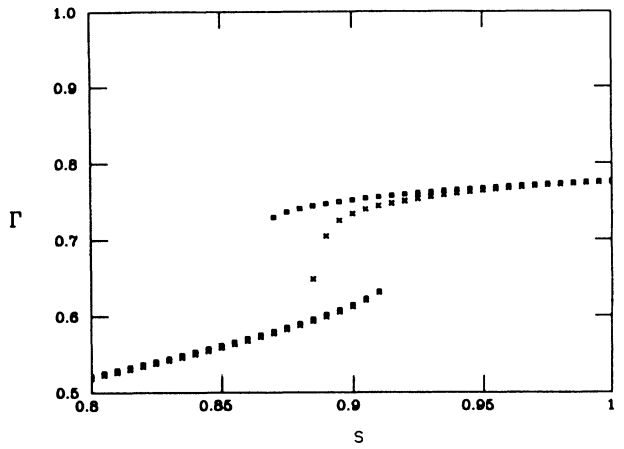

FIG. 5. Γ vs s for an infinitely long slit of width $N_z=18$ at fixed temperature $T=0.95T_c$ (squares) and for an open slit characterized by $N_z=18$ and height $L_y=140$ (crosses).

discontinuous fashion. During the adsorption process, instead, we observe a continuous thickening of the films at each wall until these reach the instability point.

We also show some isotherms obtained at $T/T_c=0.95$ and different plate separation (Figs. 5 and 6). The reduction of the plate separation N_z leads to the appearance of a critical point, close to $N_z=10$.

At lower temperatures (close or below the two-dimensional critical temperature) the fluid undergoes a sequence of layering transitions during the adsorption process, as shown in Fig. 7. Figure 8 refers to a cycle obtained by inverting the direction of change of the applied pressure slightly before the instability along the adsorption branch is reached, respectively, for the infinitely long slit and the open slit. We observe the appearance of a new kind of desorption loops, much shorter than the corresponding ones in Fig. 8. The smaller loops correspond to evaporation of layers via formation of droplets.

The infinite pore and the finite pore have adsorption branches very similar. For such a low temperature even the partially closed pore shows a pronounced hysteresis (Fig. 9). It is interesting to note that in model B the adsorption is continuous both during the emptying process and the filling. Finally, we notice the existence of smaller closed loops along the adsorption isotherm. These structures are due to the formation of menisci which acts as nucleation mechanisms for the layering transitions.

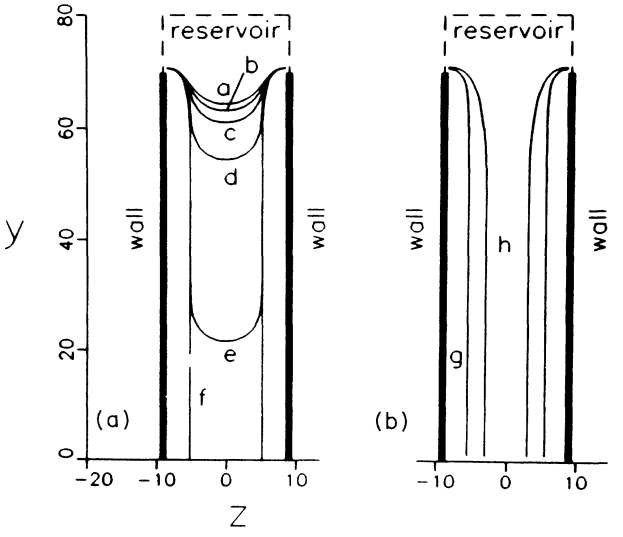

FIG. 4. Menisci obtained by plotting the density contours at fixed density $\rho=0.5$ for different values of the bulk chemical potential for $N_z=18$, $L_y=140$, $T=0.8T_c$. The menisci are labeled by latin letters: a corresponds to $s=0.921$, b to $s=0.916$, c to $s=0.911$, d to $s=0.906$, e to $s=0.903$, f to $s=0.898$. g and h obtained during the adsorption process refer, respectively, to $s=0.874$ and $s=0.975$.

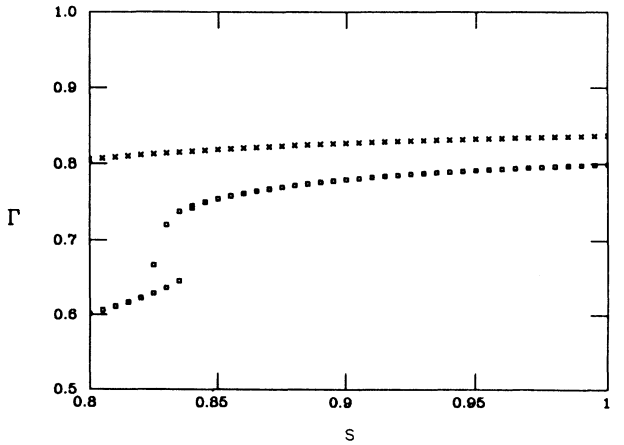

FIG. 6. Γ vs s for a slit with $N_z=14$ and $L_y=140$ at the temperature $T=0.95T_c$ (squares) and for $N_z=10$, $L_y=140$ (crosses). The absence of loops signals that the fluid in the slit is supercritical.

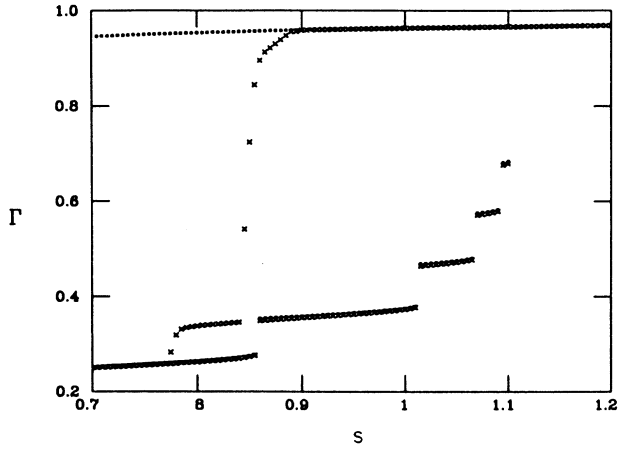

FIG. 7. Γ vs s for an infinitely long slit with $N_z=18$ at the temperature $T=0.60T_c$ (squares) and for a slit of dimensions $N_z=18$ and $L_y=140$ (crosses).

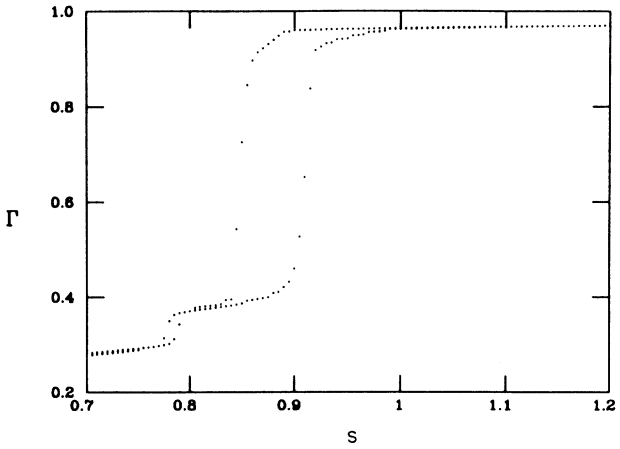

FIG. 9. Γ vs s isotherm for a partially closed slit of width $N_z=18$ and height $L_y=70$ at the temperature $T=0.60T_c$. Note the appearance of hysteresis and of a continuous adsorption branch. One also observes a smaller desorption loop at low saturation.

IV. DISCUSSION

In this section we present a discussion of the numerical results and also elucidate the mechanism which controls the filling and emptying of the pores. In order to do so we have applied semimacroscopic arguments. Let us begin by considering two types of *states* of the fluid in the pore. In Fig. 10 we show a gaslike configuration in which two liquid films of average thickness t cover the walls. In order to keep the algebra very simple, we shall assume the liquid film to have the shape of a parallelepiped of edges L_x,L_y, for the *gas* state, whereas the *liquid* configuration will be schematized by a parallelepiped of edges L_x,L_y,H. This schematization neglects the curvature of the menisci present at ends of the pore, however, provides the right qualitative picture. The present analysis is a straightforward generalization of the one performed by Evans and one of the authors.[10]

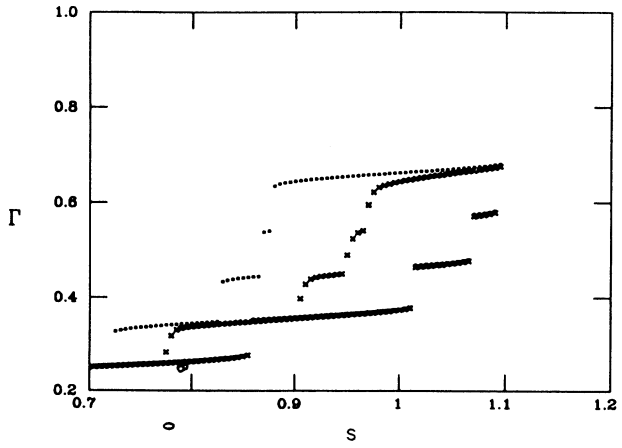

FIG. 8. Γ vs s for an infinitely long slit of width $N_z=18$ at the temperature $T=0.60T_c$, obtained by inverting the direction of change of the applied pressure during the adsorption process at $s=1.1$ (squares) and for an open slit of width $N_z=18$ and length $L_y=140$ at the temperature $T=0.60T_c$ (crosses).

For the *gas* configuration the grand potential is minimized with respect to t, the thickness of the wetting layer. This is an extension of the so called sharp-kink approximation which is well known as Frenkel-Halsey-Hill slab model for an adsorbed film. The criterion for two phase coexistence in the pore, is obtained by comparing the grand potential relative to the *gas* state with that of the *liquid* state. One finds the following equilibrium condition at fixed chemical potential:

$$P_{\text{gas}}-P_{\text{liquid}}=2\gamma[1-(H-2t)/L_y]/(H-2t)\ , \quad (4.1)$$

where P_{gas} and P_{liquid} are, respectively, the pressure of the gas and of the liquid at given μ. Long-ranged dispersion forces, due to the walls, should also be included in the grand potential of the film and they contribute a term proportional to $1/t^2$, modifying Eq. (4.1) in the following way:

$$P_{\text{gas}}-P_{\text{liquid}}=2\gamma[1-(H-2t)/L_y]/(H-3t)\ . \quad (4.2)$$

Thus the presence of the menisci has the effect of shifting the first-order transition by a factor proportional to H/L_y toward bulk coexistence, with respect the infinitely long pore case ($L_y=\infty$). A critical point is also expected: as the temperature increases, at fixed plate separation, the two states will coalesce determining what has been termed a capillary critical point.[6] The instability criterion for the film during the adsorption process has been obtained by several authors before.[7,19,20] Two approaches have been exploited and both give the same answer. Saam and Cole performed an hydrodynamic analysis of the stability of the film under small perturbations. The other approach is best based on density functional methods. According to these theories, in the case of long-ranged dispersion forces, the thickness of the film grows as[21]

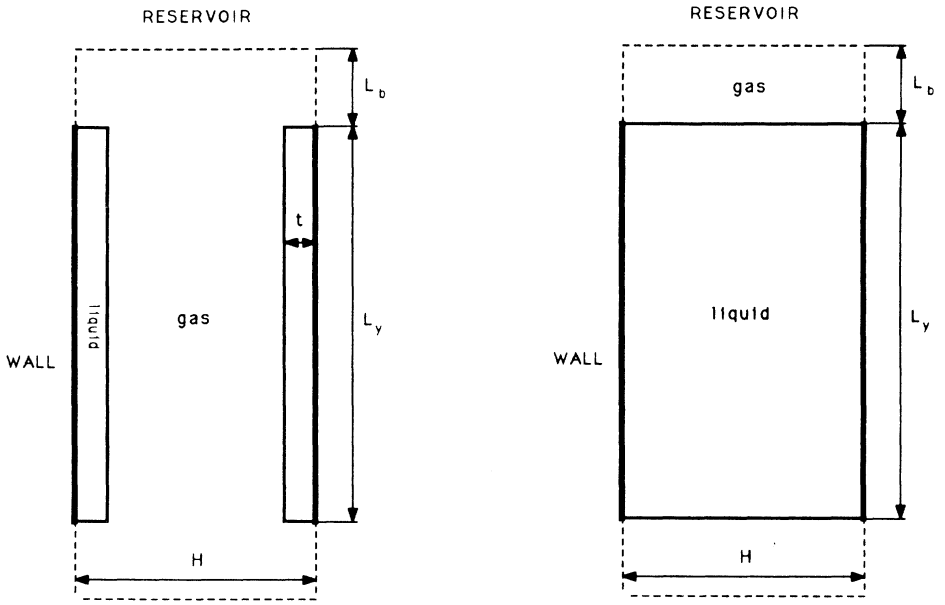

FIG. 10. Schematic visualization of the gaslike configuration in a complete wetting situation (left) and of the liquidlike configuration (right).

$$t \sim (P_{\text{gas}} - P_{\text{liquid}})^{-1/3} .$$

On the approach to bulk coexistence the difference on the right-hand side vanishes and t becomes greater than $H/2$ giving a completely filled pore. In contrast, the mechanism for desorption is different from the ones proposed in the past on the basis of microscopic arguments.

When $P > P_{\text{cond}}$ the pore is full, two slightly curved menisci are present, as illustrated in Fig. 4. As $P \sim P_{\text{cond}}$, which is the value at which a gaslike and a liquidlike configuration coexist in the infinitely long pore case, the wetting layers are nucleated at the open ends and the menisci start to recede at an increasing rate towards the interior of the capillary. For P slightly less than P_{cond} the equilibrium configuration in the open pore is nonuniform in the vertical direction and looks like a superposition of the two configurations observed in the infinitely long pore with a region in between joining them. This is the meniscus, i.e., the analog of the liquid-vapor planar interface in an infinite system at two phase coexistence. The receding of the meniscus is a consequence of the growth of a new phase which *wets* the system, the reservoir playing the role of spectator phase. The presence of lateral walls makes this wetting process nonuniform in more than one direction. We shall analyze in the Appendix the desorption mechanism in more detail, with the help of a toy model.

We compare, now, with the traditional macroscopic description[22] of condensation. On the grounds of surface thermodynamics, the equilibrium pressure P_{gas} over a concave meniscus of liquid must be larger than the pressure of the liquid P_{liquid} at the same temperature and chemical potential. The difference in pressure is related to the mean radius of curvature r_m of the meniscus through the equation

$$P_{\text{gas}} - P_{\text{liquid}} = 2\gamma(\cos\theta)/r_m , \tag{4.3}$$

where θ is the so-called contact angle. For practical reasons one favors a different form of Eq. (4.3). This is obtained by expanding to first order the pressure difference in powers of $\Delta\mu = \mu - \mu_{\text{coex}}$ and treating the vapor as an ideal gas

$$\ln(P/P_{\text{coex}}) = -2\gamma(\cos\theta)/[k_B \text{Tr}_m (n_{\text{liquid}} - n_{\text{gas}})] .$$

The filling takes place at the relative pressure obtained by inserting for $r_m = 2(1/r_1 + 1/r_2)^{-1}$ the value of the ad-

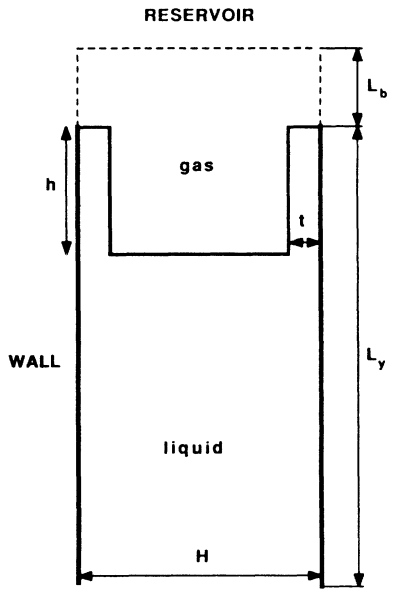

FIG. 11. Toy model density profile employed in the Appendix.

sorption radius r_m^{ads}. For a very wide slit r_m^{ads} is approximately infinite (there is no curvature, the film being planar) and the nucleation process occurs very close to bulk coexistence.

On the other hand, the inverse process of emptying occurs via evaporation at the hemispherical menisci present at each end. The pressure at which the emptying takes place is determined by the radius of curvature of the meniscus, whose value is given by $r_m^{des}=(H-2t)$. Upon substituting the above value of the mean radius in the Kelvin equation one can read off a value of the pressure, which is close to the one at which condensation occurs in the infinitely long pore. This value of the pressure for the emptying process is in agreement, for wide slits, with the numerical prediction of the model here proposed.

V. CONCLUSIONS

In this paper we have addressed the long-standing open problem of constructing a microscopic theory, which is capable of describing the hysteresis phenomena in porous media. In order to achieve this goal we have introduced a new model of pore, schematized by an open slit and applied the density-functional formalism.

The presence of free surfaces is seen to have dramatic consequences. In contrast with the unbounded parallel-plate case, previously employed in earlier studies, the desorption process is not due to spinodal decomposition, but to heterogeneous nucleation induced by the presence of nonuniform walls.

The new mechanism provides a possible explanation for the absence of very long desorption branches, observed in recent experiments.[23] We cannot rule out the possibility that other mechanisms, such as dynamical effects, might be responsible for this phenomenon. However, to the best of our knowledge, the present explanation is the first microscopic account of the fact that the desorption process occurs very close to the first-order transition. In our study, the new phase, i.e., the gas, appears at the end of the pore in a continuous fashion and grows at an increasing rate at the expenses of the liquid. We have visualized this growth by showing the menisci for different saturations.

We remark that the location of the equilibrium first order transition is not strongly affected by the finite length of the pore. Thus the present work successfully bridges the gap between the classic approach to capillary phenomena (the meniscus theory) and the modern microscopic density-functional approach recently introduced. How valid is the above picture of hysteresis, based on the mean-field approximation? For the infinitely long pore there exist a thorough comparative study between MFA results and computer simulation, which shows a remarkable agreement between these methods.[24] In particular the extension of the spinodals is comparable. Fluctuations, as it is well known, cause the critical exponents calculated within the MFA to be not exact and also produce a shift of the phase diagram. However, we strongly believe that the nucleation mechanism, we have introduced, would act in an analogous manner even in the presence of fluctuations, not being these alone capable to modify any relevant aspect of the above scenario.

ACKNOWLEDGMENTS

One of the authors (U.M.B.M.) wishes to thank A. Fernandez, J. Pech and A. Tarancon for their help with TEX and L. Pietronero for reading the manuscript. Research supported by the Istituto Nazionale di Fisica Nucleare, Sezione di Roma.

APPENDIX

It remains to ascertain the desorption behavior in the limit of very long open slits ($L_y \to \infty$); this goal is achieved by resorting to a very simple parametrization of the density profile, as illustrated below. We schematize the density distribution $n(y,z)$ by means of a function which can take up only two values n_{liquid} and n_{gas}. This assumption is a straightforward generalization of the slab model often employed to study interfacial problems. When the emptying process is already in its developed stage, the study above shows that the liquid fills completely the inner part of slit while two liquid films creep over the walls. A gaslike region is present between the two liquid films, while a meniscus is present in the zone where the two films merge together. Neglecting the curvature of this meniscus, we assume the trial density profile shown in Fig. 11. For algebraic convenience we employed in this section continuous fluid-fluid and substrate-fluid interactions, of the exponential Yukawa potential type,[25]

$$w(r)=-\alpha\lambda^2\frac{\exp(-\lambda r)}{(4\pi r)} \ . \tag{A1}$$

The grand potential associated with such a trial density profile is easily obtained. Upon neglecting small terms it can be written as

$$\frac{\Omega}{L_x}=-P_{\text{liquid}}[2th+H(L_y-h)]-P_{\text{gas}}(H-2t)h+\gamma(H+2h)+\frac{2\varepsilon_w}{\lambda}(n_{\text{liquid}}-n_{\text{gas}})\exp(-\lambda t)h$$
$$+\frac{2\varepsilon_w}{\lambda}n_{\text{liquid}}L_y+\frac{2\varepsilon_{\text{res}}}{\lambda}(n_{\text{liquid}}-n_{\text{gas}})(\{1-\exp[-\lambda(h+L_b)]\}(H-2t)+[1-\exp(-\lambda L_b)]2t) \ , \tag{A2}$$

where $\gamma=\alpha(n_{\text{liquid}}-n_{\text{gas}})^2/4\lambda$ is the liquid-gas surface tension within the sharp-kink approximation. The equilibrium value of Ω is obtained by minimizing with respect to h and t. Thus we find in the limit of h and L_y large

$$\lambda t=-\ln\{(P_{\text{gas}}-P_{\text{liquid}})/[(n_{\text{liquid}}-n_{\text{gas}})\varepsilon_w]\} \tag{A3}$$

and

$$\lambda(h+L_b)=-\ln\{[P_{\text{gas}}-P_{\text{liquid}}-2\gamma/(H-2t)]/[(n_{\text{liquid}}-n_{\text{gas}})\varepsilon_{\text{res}}]\}\ , \tag{A4}$$

where ε_w measures the wall strength and ε_{res} is the wall strength of the boundaries of the reservoir. Equation (A3) gives the thickness of the wetting film as a function of the pressure difference of the two phases, whereas Eq. (A4) yields an expression for the location of the meniscus as a function of the distance from the equilibrium first order phase transition. Note, in fact, that as $(P_{\text{gas}}-P_{\text{liquid}})\to 2\gamma/(H-2t)$ (this occurs on the approach to capillary coexistence from the liquid side) the value of h grows, i.e., the meniscus empties. Thus monitoring the position h of the meniscus is equivalent to monitor the adsorption. Formula (A4) explains why the emptying of the meniscus occurs in a narrow interval close to the condensation point. We remark that the logarithmic character of the law found above is a detail, which depends on the type of wall potential we employed.

[1]A. Zsigmondy, Z. Anorg. Chem. **71**, 356 (1907).

[2]L. H. Cohan, J. Am. Chem. Soc. **60**, 433 (1983).

[3]J. S. Rowlinson and B. Widom, *Molecular Theory of Capillarity* (Clarendon, Oxford, 1982).

[4]D. E. Sullivan and M. M. Telo da Gama, *Fluid Interfacial Phenomena,* edited by C. A. Croxton (Wiley, New York, 1986).

[5]S. Dietrich, in *Phase Transitions,* edited by Domb and Lebowitz (Academic, New York, 1988), Vol. 12.

[6]R. Evans, U. Marini Bettolo Marconi, and P. Tarazona, J. Chem. Phys. **84**, 2376 (1984).

[7]R. Evans, U. Marini Bettolo Marconi, and P. Tarazona, J. Chem. Soc. Faraday Trans. 2 **82**, 1763 (1986).

[8]P. Tarazona, U. Marini Bettolo Marconi, and R. Evans, Mol. Phys. **60**, 573 (1987).

[9]R. Evans and U. Marini Bettolo Marconi, J. Chem. Phys. **86**, 7138 (1987).

[10]R. Evans and U. Marini Bettolo Marconi, Chem. Phys. Lett. **114**, 557 (1985).

[11]P. C. Ball and R. Evans, Mol. Phys. **63**, 159 (1988).

[12]P. C. Ball and R. Evans, Europhys. Lett. **4**, 715 (1987).

[13]T. L. Hill, J. Chem. Phys. **15**, 767 (1947).

[14]M. J. De Oliveira and R. B. Griffiths, Surf. Sci. **71**, 687 (1978).

[15]D. Nicholson, J. Chem. Soc. Faraday Trans. 1 **72**, 29 (1976).

[16]E. Bruno, U. Marini Bettolo Marconi, and R. Evans, Physica A **141**, 187 (1987).

[17]R. Evans, Adv. Phys. **28**, 143 (1979).

[18]For a cylindrical pore this width will be reduced by a factor of 2, because of the effects due to the curvature.

[19]W. F. Saam and M. W. Cole, Phys. Rev. B **11**, 1086 (1975).

[20]M. W. Cole and W. F. Saam, Phys. Rev. Lett. **32**, 985 (1974).

[21]In the case of a cylinder the instability is shifted by the presence of a curvature term $t\sim(P_{\text{gas}}-P_{\text{liquid}}-\gamma/R)^{-1/3}$, where R is the radius of the cylinder. Thus one observes narrower loops in this case.

[22]S. J. Gregg and K. S. W. Sing, *Adsorption, Surface Area and Porosity* (Academic, New York, 1982).

[23]D. D. Awschalom, J. Warnock, and M. W. Shafer, Phys. Rev. Lett. **57**, 1607 (1986).

[24]B. K. Peterson, K. E. Gubbins, G. S. Heffelfinger, U. Marini Bettolo Marconi, and F. Van Swol, J. Chem. Phys. **80**, 6487 (1988).

[25]D. E. Sullivan, Phys. Rev. B **20**, 3991 (1979).